13th World Conference on Earthquake Engineering
Vancouver, B.C., Canada
August 1-6, 2004
Paper No. 2785

SOIL FRICTION RESTRAINT OF OBLIQUE PIPELINES IN DENSE SAND

TUNG-WEN HSU[1], YUH-JYH CHEN[2] and WAY-CHANG HUNG[3]

SUMMARY

The soil restraint on pipelines due to oblique relative movement between the pipeline and dry dense sand was investigated. Model pipes 0.61 m long with diameters of 152.4, 228.6, and 304.8 mm are obliquely moved from an axial-longitudinal to lateral-transversal direction in the large scale drag box to study the associated soil friction restraint of the oblique pipes in the shallow buried depth. All the experimental results indicated that the longitudinal soil restraint of the axial pipes could be estimated as the product of the average of the vertical and horizontal earth pressure at the centerline of the pipe and the tangent value of soil-pipe friction angle. For the lateral pipes, three different theoretical methods were used to analyze the experimental results. Among these, the modified Meyerhof's theory deriving for the bearing capacity of foundation was applied to estimate the transversal soil restraint. It was found that the modified Meyerhof's approach with the assumption of the rupture surface of logarithmic spiral arc was more closely to the experimental results comparing with the planar sliding surface. For the oblique angle pipes, the longitudinal soil restraint decreases, whereas the transversal soil restraint increases with the oblique angle, respectively. Moreover, the longitudinal and transversal soil restraint of the oblique angle pipes could be obtained by multiplying the corresponding cosine and sine values of the oblique angle with the associated longitudinal soil restraint of axial pipe and the transversal soil restraint of the lateral pipe, respectively. The findings also indicate that the scale effects are minor for the size up to 304.8 mm of the pipe diameter tested herein.

INTRODUCTION

Underground pipelines are extensively used to carry oil and gas from their deposit to the consumption places. An understanding of soil restraint on pipelines due to the soil-pipe relative movement is important for the pipeline designers. The soil friction restraint on the pipelines in the longitudinal-axial direction is one of the four principal subjects needed to be investigated as noted by Nyman [1]. O'Rourke et al. [2] pointed out that most of the earthquake damage to buried pipelines has been attributed to the surface wave propagation and the permanent ground deformation (PGD). In studying the seismic wave propagation

[1] Prof., Dept. of Civil Engrg., Nat'l Chung-Hsing Univ., Taichung, Taiwan. twhsu@dragon.nchu.edu.tw
[2] Research Associate, formerly Ph.D. Student, Dept. of Civil Engrg., Nat'l Chung-Hsing Univ., Taichung, Taiwan. chenyj@ms21.url.com.tw
[3] Graduate Student, Dept. of Civil Engrg., Nat'l Chung-Hsing Univ., Taichung, Taiwan.

effects on buried pipeline, O'Rourke and El Hmadi [3] estimated that the strain in the pipeline was induced by friction force at the soil pipeline interface. In their analysis, the soil friction restraint per unit length of pipeline at the interface is dependent on the coefficient of friction at the soil-pipeline interface. In addition, O'Rourke et al. [2] found that the earthquake-induced wrinkling damage to steel pipe in the 1985 Mexico City was due to the longitudinal PGD. Strain induced in the pipelines subjected to the longitudinal PGD is through the friction-like forces at the soil-pipe interface. To estimate the friction force, O'Rourke and El Hmadi [3] used the experimental results done by Brumund and Leonards [4], in which the maximum forces per unit length at the soil-pipe interface f_m is equal to the multiplication of the coefficient of friction μ between the surrounding sand and pipeline, as well as the product of the circumference and the average of the vertical and horizontal earth pressure on the pipe, which could be expressed as follows:

$$f_m = \mu\gamma z\left(\frac{1+\kappa_0}{2}\right)\pi D \quad (1)$$

where γ = unit weight of the soil; z = distance measured from the pipeline centerline to the ground surface; k_0 = coefficient of lateral earth pressure at rest; and D = diameter of the pipeline. The coefficient of friction μ varies between $0.5\tan\varphi$ and $1.0\tan\varphi$ depending on the pipeline surface condition, where φ is the internal friction angle of the soil. In examining the above equation, it was found that the coefficient of friction for various pipe surface conditions was described by the different magnitude of $\tan\varphi$. The soil–pipe friction angle, which is frequently adopted by the geotechnical engineers (Terzaghi et al. [5]), is not presented. In general, the in-placed pipelines are not always installed in such a way that their orientation is always parallel to the direction of the longitudinal PGD. The oblique pipelines subjected to the impact with the combination of transversal PGD and longitudinal PGD would be frequently occurred in the field. Therefore, it becomes pertinent to perform experimental tests to measure the longitudinal soil restraint as well as the associated transversal soil restraint on the oblique pipelines. The behavior of soil restraint on pipelines depends on the surrounding soil density and the mode of loading, namely, transversal and longitudinal where the pipelines are encountered. Early study (Hsu, et al. [6]) shows that the transversal soil restraint of oblique angle pipes could be predicted by using the limit equilibrium model with the assumption of the planar failure surface. This research continues the previous study to investigate the possible different failure mechanism of the oblique motion pipes developed in dense sand. Same variables such as pipe oblique angle, recess depth, and diameter of the pipe are included in this study. The inclination angles, α, ranging from 0º for pure axial to 90º for pure lateral pipe motion are

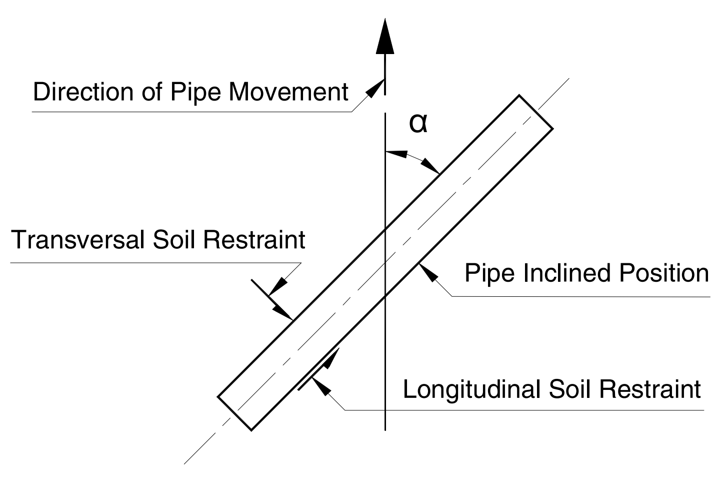

Fig. 1. Sketch of Pipe Oblique Angle α

defined as shown in Fig. 1. Three sizes of pipe with diameters of 152.4 mm (6 in.), 228.6 mm (9 in.) and 304.8 mm (12 in.) were used. The shallow burial depths H/D ranged from 1 to 3 were tested, in which H is the recess depth of the pipe measured from the sand surface to the centerline of the pipe and D is the diameter of the pipe. Local sand from the Da-Du riverbed in the central area of Taiwan was used for all tests. Dense sand with a density of 17.16 kN/m^3 (1.75 g/cm^3), corresponding with the direct shear internal friction angle of 42° (relative density of 94%), was prepared in this investigation. The exterior surface roughness of the pipes was that of a normal exposed pipe. The soil-pipe friction angle was about 26°. All the pipe loading tests were performed in a prefabricated large-scale drag box with internal dimensions 1.83 m × 1.83 m × 1.22 m (6 ft × 6 ft × 4 ft). The movement and the oblique angle of the pipe were controlled by the rotation of the lead screw actuated by the horizontal and vertical drive motors simultaneously. The components of the test apparatus are schematically shown in Figs. 2 (a, b, and c). The detailed description of the experimental setup can be found elsewhere in a companion paper (Hsu et al. [6]).

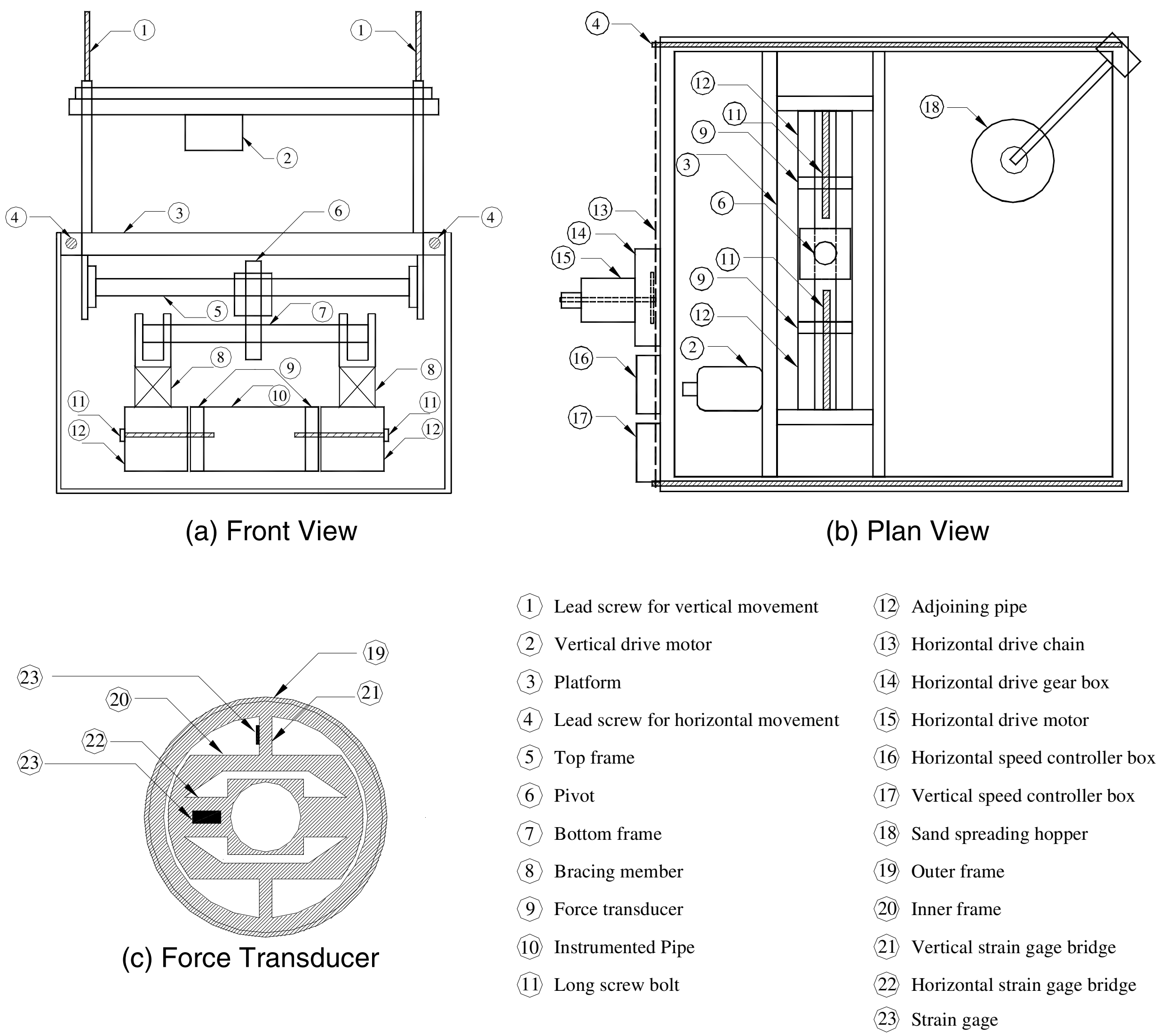

Fig. 2. (a)(b) Cross Section of Large Scale Drag Box and (c) Force Transducer Measurement System.

RESULTS

Ultimate Resistance

For each oblique pipe loading test, the associated transversal soil force F_H and longitudinal soil force F_V will be imposed on the pipe as shown in Fig. 1. Typical results of the force-displacement curves for the oblique motion pipe are shown in Figs. 3 (a and b), respectively. In the figures, the results have been plotted as the dimensionless transversal force $F_H/(\gamma HDL)$ or dimensionless longitudinal force $F_V/(\gamma HDL)$ versus dimensionless displacement Y/D, in which L = the pipe length; Y = the pipe displacement; and the other variables are the same as previously defined. As shown in Fig. 3a, the dimensionless ultimate transversal force was defined at the point where the force-displacement curve reached a well-defined peak, whereas the dimensionless ultimate longitudinal force was selected at the point where the force-displacement starts to level off as illustrated in Fig. 3b. Arrows on the curves show the points representing the dimensionless ultimate transversal force F'_{HM} denoted as $F'_{HM} = F_{HM}/\gamma HDL)$ or the dimensionless ultimate longitudinal force F'_{VM} denoted as $F'_{VM} = F_{VM}/(\gamma HDL)$, in which F_{HM} and F_{VM} are the ultimate transversal and longitudinal forces, respectively. It could be observed that F'_{HM} and F'_{VM} might occur approximately at the same pipe displacement in dense sand. The results also indicate that F'_{HM} increased, whereas F'_{VM} decreased with the oblique angle. Most of the increase in F'_{HM} is associated with the oblique angles in the interval between 0º and 45º, however, the majority of the decrease in F'_{VM} is corresponding with the oblique angles between 45º and 90º.

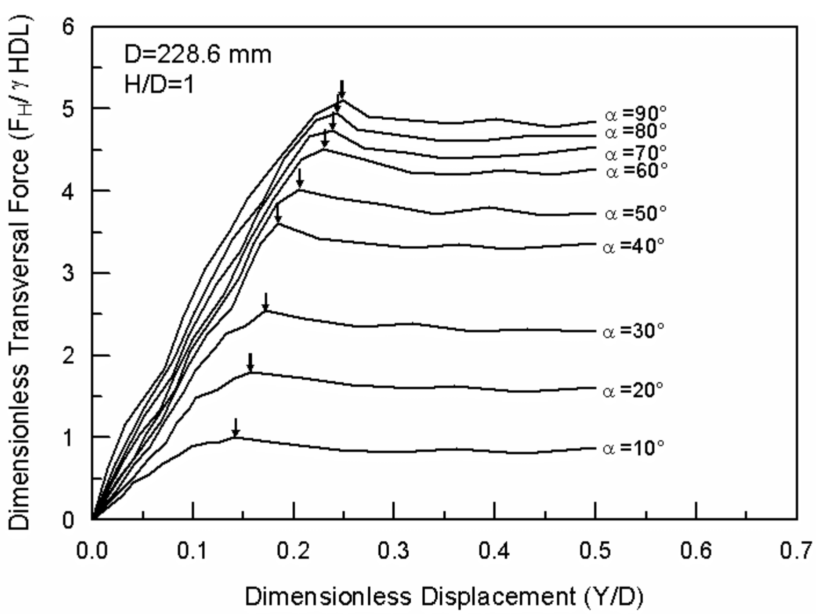

(a)

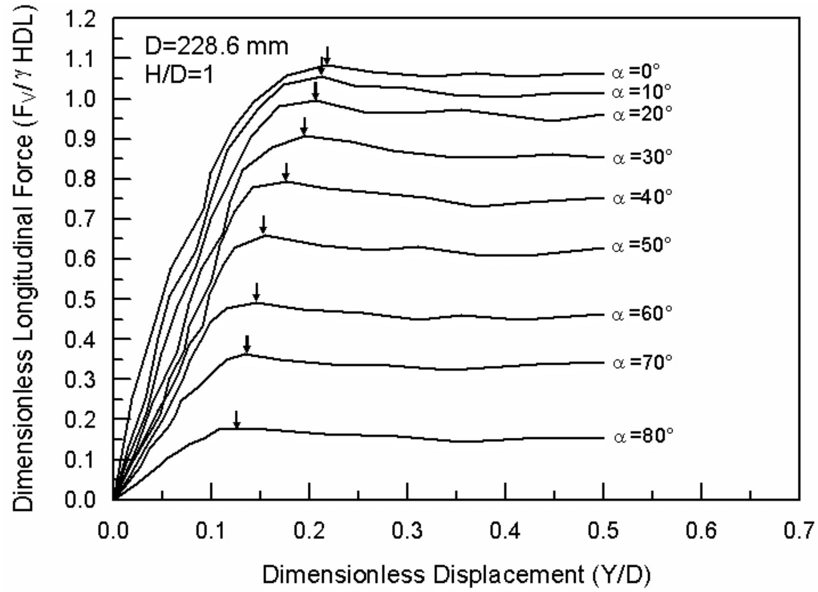

(b)

Fig. 3. Dimensionless Displacement Y/D for 228.6-mm Pipe with *H/D* = 1 verse: (a) Dimensionless Transversal Force $F_H/\gamma HDL$; (b) Dimensionless Longitudinal Force $F_V/\gamma HDL$

Theoretical Analysis

Transversal Soil Restraint of Lateral Pipelines ($\alpha = 90^o$)

The behavior of transversal soil restraint on lateral pipelines in sand depends on the surrounding soil density and the burial depth of the pipes as noted by Audibert and Nyman [7]. Through the glass window view of the failure surface developed in the pipe loading test, it was found that the failure mechanics of shallow burial pipe with *H/D*< 3.5 consisted of a narrow vertical active zone formed on the top of the pipe and a passive wedge bounded by a logarithmic spiral developed in front of the pipe. For analytical purposes, three theoretical approaches with different failure mechanics, namely, planar failure surface, logarithmic spiral failure surface, and the modified Meyerhof's theory of logarithmic spiral failure surface were discussed as follows.

Planar Failure Surface

The failure mechanism of planar failure surface was originally developed by Nyman [7]. In which, an analog between the resistance of the anchor plate and the restraint of pipeline was made and a sliding plane surface was assumed in front of the pipe for simplifying its analysis. Besides, Nyman [7] proposed a model to estimate the transversal soil restraint by using the implicit limit equilibrium. The writers modified the Nyman's approach by placing the projected anchor plate at the centerline of the pipe instead of at the front edge of the pipe (Hsu et al. [6]). For the lateral pipes subjected to the horizontal motion, the limit equilibrium model together with the force polygon in the soil wedge are shown in Figs. 4(a and b), respectively.

The forces in the soil wedge are as follows: R_1 is the resultant of the lateral earth pressure at active stress state acting on the left side of soil wedge; W is the soil weight embodied within the soil wedge; and R_2 is the resultant of the shear and normal forces acting on the passive sliding surface. For determining the transversal soil restraint of the lateral pipeline, the trial sliding surface with varying angles θ is repeated until the minimum value of P_u is reached as shown in Fig. 4(b). The value of P_u could also be solved through the following matrix form.

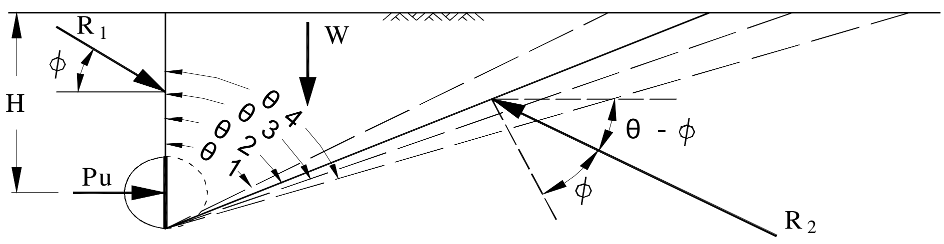

(a)

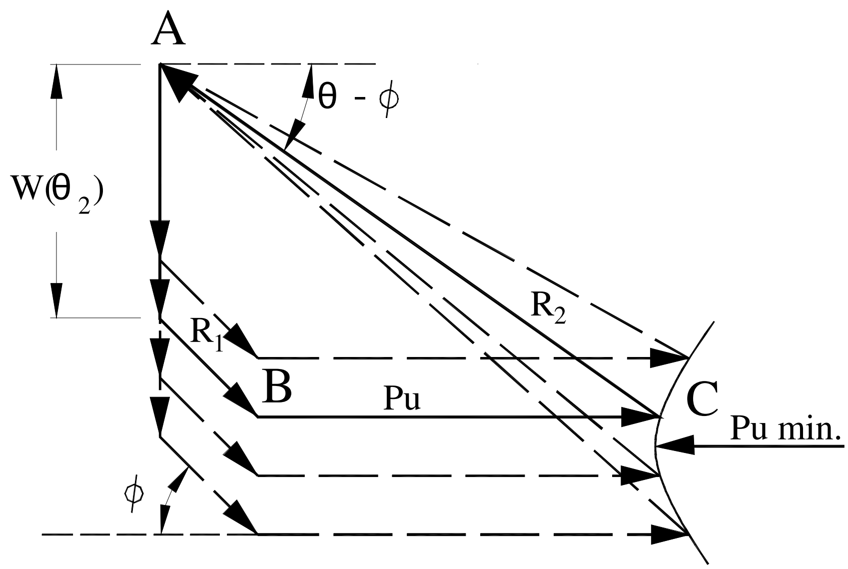

(b)

Fig. 4 Implicit Limit Equilibrium Model with Planar Failure Surface: (a) Limit Equilibrium Model; (b) Equilibrium of Force Polygon

$$\begin{bmatrix} 1 & -\cos(\theta-\phi) \\ 0 & \sin(\theta-\phi) \end{bmatrix} \begin{bmatrix} p_u \\ R_2 \end{bmatrix} = \begin{bmatrix} -R_1\cos\phi \\ W+R_1\sin\phi \end{bmatrix} \tag{2}$$

Logarithmic spiral failure surface

Typical form of the logarithmic spiral failure surface in pipe loading test is shown in Fig. 5a. Similar to the passive earth pressure developed on the retaining wall, the curved lower portion CD of the failure surface is assumed to be an arc of a logarithmic spiral. And the center of the arc lies on the line BD which makes an angle of (45-φ/2) degrees with the horizontal. Beyond curve CD, the straight upper portion DD' is in the zone of the Rankine passive state.

To evaluate the ultimate soil restraint P_u on the pipeline, the trial wedge procedures outlined by Terzaghi et al. [5] was used as shown in Fig. 5a. An arbitrarily selected sliding surface CDD' consists of the logarithmic spiral CD with its center at O lying along the straight line BD' which makes an angle of (45-φ/2) with the horizontal. Considering all the forces on the free body of the soil wedge ACDF on sliding failure surface CDD' as illustrated in Fig. 5b, the corresponding P_u value could be obtained by taking moment of all the forces on the free body ACDF about O. All the forces on the free body ACDE are as follows: W_1 is the soil weight of the rectangular area ABEF; W_2 is the soil weight of the triangular area BDE; W_3 is the soil weight of the sector area OCD; W_4 is the soil weight of the triangular area BOC; W_5 is the soil weight of the half area of the pipe; R_1 is the resultant of the lateral earth pressure at active stress state acting at the lower third-point of AB; and R_2 is the passive earth pressure acting at a distance of FD/3 measured vertically from D; and R_3 is the resultant of the shear and normal forces that act along the surface of sliding CD which makes an angle φ with the normal to the spiral at its point of application and passes through the point O. Taking moment of all the above forces with respect to point O, it yields.

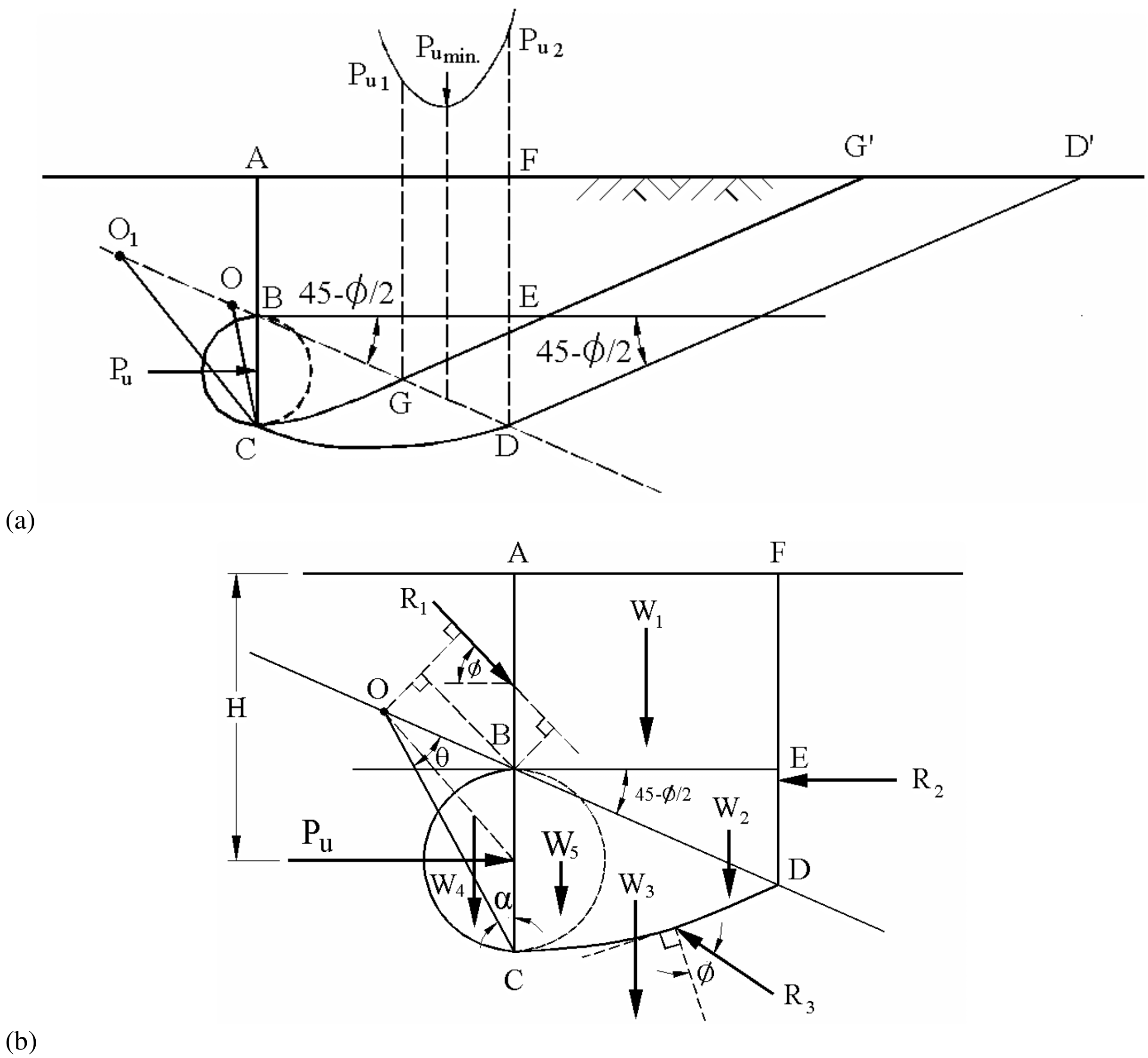

Fig. 5 Logarithmic Spiral Failure Surface (a) Trial Failure Wedge; (b) All Forces Acting on Soil Mass ABCD.

$$P_u \cdot L_{P_u} = W_1 \cdot L_{W_1} + W_2 \cdot L_{W_2} + W_3 \cdot L_{W_3} - W_4 \cdot L_{W_4} - W_5 \cdot L_{W_5} + R_1 \cdot L_{R_1} + R_2 \cdot L_{R_2} \quad (3)$$

Where L_{P_u}, L_{w_1}, L_{w_2}, L_{w_3}, L_{w_4}, L_{w_5}, L_{R_1}, and L_{R_2} are the corresponding moment arms for the forces P_u, W_1, W_2, W_3, W_4, W_5, R_1, and R_2, respectively. The preceding procedure for finding the trial ultimate soil restraint P_u is repeated for several trial wedges until P_u value converges to a minimum.

Modified Meyerhof's theory of logarithmic spiral failure surface

This method was originally developed by Meyerhof for deriving the bearing capacity of foundation under vertical loads (Meyerhof [8]) and inclined loads (Meyerhof [9]). After some modification, the analytical procedures were described as follows. The failure zone under the lateral pipeline loading includes the Rankine active zone ABF, plane shear zone BEF, radial shear zone BDE, and the elastic zone BCD, respectively as shown in Fig. 6.

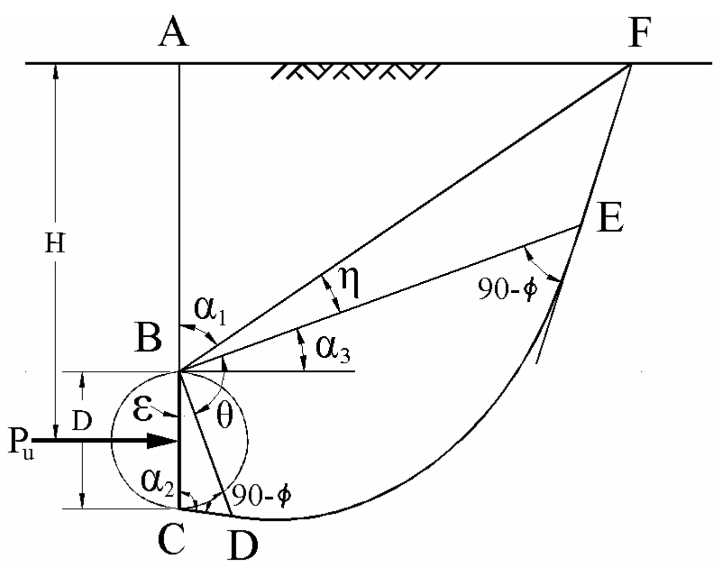

Fig. 6 Modified Meyerhof's Logarithmic Spiral Failure Surface

To estimate the ultimate soil restraint P_u on the pipeline, the analytical procedures start from the active stress zone ABF for the trial failure surface CDEF. Fig. 7a shows all the forces acting on the Rankine active stress zone ABF. In the soil wedge ABF, R_0 is the resultant of the lateral earth pressure at active stress state acting on the left side of the soil wedge; W_0 is the soil weight embodied within the soil wedge; and σ_0 and τ_0 are the normal stresses and the shear stresses acting on the boundary BF, respectively. The σ_0 and τ_0 values could be determined from the conditions of force equilibrium in the directions of x'-axis and y'-axis, respectively as shown in Fig. 7a.

$$\tau_0 \cdot \overline{BF} = -R_0 \cdot \sin(90 - \phi + \alpha_1) + W_0 \cdot \cos\alpha_1 \quad (4)$$

$$\sigma_0 \cdot \overline{BF} = -R_0 \cdot \cos(90 - \phi + \alpha_1) + W_0 \cdot \sin\alpha_1 \quad (5)$$

After obtaining σ_0 and τ_0 values, the normal stresses σ_1 on BE in the plane shear zone BEF could be determined from the force equilibrium in the Y"-axis direction as shown in Fig.7b.

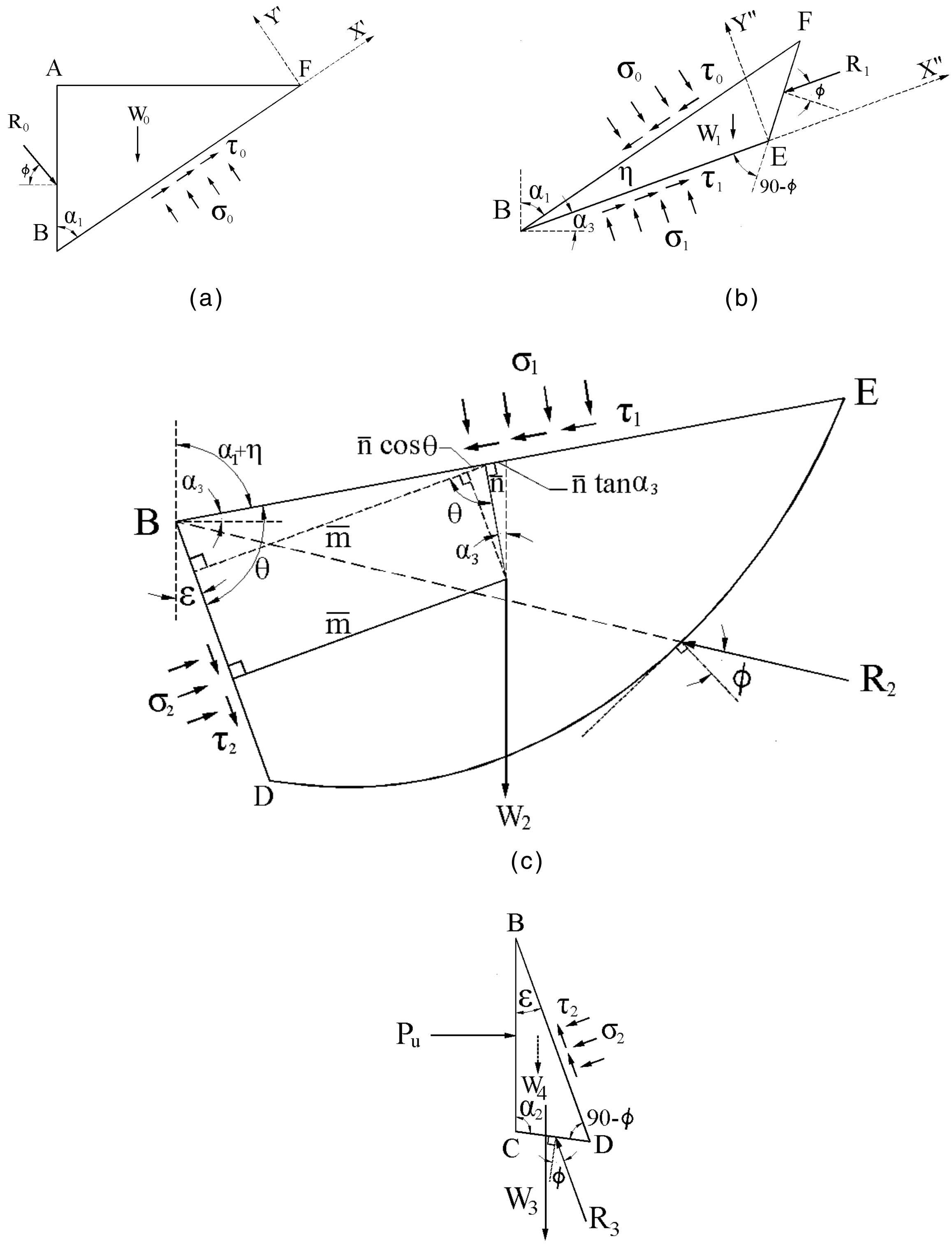

Fig. 7 Modified Meyerhof's Theory (a) Stresses Acting on Rankine Active Zone; (b) Stresses Acting on Plane Shear Zone; (c) Stresses Acting on Radial Shear Zone; (d) Stresses Acting on Elastic Zone.

$$\sigma_1 \cdot \overline{BE} = \tau_0 \cdot \overline{BF} \cdot \sin\eta + \sigma_0 \cdot \overline{BF} \cdot \cos\eta + W_1 \cdot \cos\alpha_3 \tag{6}$$

Where W_1 is the soil weight of the plane shear zone area BEF; η is the angle between BF and BE, which are the boundaries of the plane shear zone; and $\alpha_3 = \varepsilon + \theta - 90°$ in which ε and θ are the angles denote the elastic zone and the radial shear zone of the failure surface as shown in Fig. 6. With the determined σ_1 value, the normal stresses σ_2 on BD as shown in Fig. 7c could be obtained by taking moment of all the forces on sector zone BDE with respect to point B as follows.

$$\sigma_2 = \left(\frac{\overline{BE}}{\overline{BD}}\right)^2 \cdot \sigma_1 + \frac{2 \cdot W_2 \cdot L_{W2}}{\overline{BD}^2} \tag{7}$$

Where W_2 is the soil weight of the sector zone area BDE; L_{w_2} is the moment arm for the soil weight W_2, which can be computed through the centroid of the spiral section BDE. After obtaining the σ_2 value, the lateral soil restraint P_u could be calculated through the force equilibrium in the P_u and perpendicular to P_u directions as shown in Fig. 7d. After manipulation, it yields.

$$P_u = \sigma_2 \cdot \overline{BD} / \cos\varepsilon + (W_3 - W_4)\tan\varepsilon \tag{8}$$

In which W_3 is the soil weight of the elastic zone BCD; W_4 is the soil weight of the half area of the pipe; and ε is the angle between BC and BD. The magnitude of P_u can then be minimized with respect to independent admissible variations of ε and θ.

Longitudinal Soil Restraint of Axial Pipeline ($\alpha = 0°$)

The longitudinal soil restraint f_m of axial pipeline ($\alpha = 0°$) could be determined from equation (1), in which the coefficient of friction μ between sand pipeline needs to be estimated. To do this, the soil-pipe friction angle δ was determined through the direct shear test, which was about 26°. The value of μ was then expressed as $tan\delta$. As well, the k_0 value was computed as the coefficient of lateral earth pressure at rest, which was equal to ($1\text{-}sin\varphi$).

Scale Effects of Pipe Diameter

To study the scale effects of pipe diameter on the dimensionless ultimate transversal force F'_{HM} and the dimensionless ultimate longitudinal force F'_{VM}, all the test results of different size pipes at the same burial depth were grouped together as shown in Figs. 8a and 8b, and Figs. 9a and 9b, respectively. It was found that the scale effects were minor for pipe diameter up to 304.8 mm (12 in.) in this series of experimental tests.

Comparison with Theoretical Predictions

The foregoing theoretical analysis was studied primarily on the associated soil restraints of oblique pipes oriented at ($\alpha = 0°$) and ($\alpha = 90°$), respectively. Based on the force equilibrium, the transversal soil restraint of the oblique angle pipe could be geometrically obtained by multiplying the corresponding sine value of the oblique angle with the transversal soil restraint of the lateral pipe ($\alpha = 90°$). Figs. 8a, 9a, and 10a show the comparison between the theoretical predictions of three different analyses with the experimental results. It can be observed that the difference among these three methods is minor for shallow burial depth up to $H/D = 2$ and all three predicted values are in good agreement with the experimental results as shown in Figs. 8a and 9a, respectively. However, as the burial depth becomes deep at $H/D = 3$, the planar failure surface gives increasingly overestimated values comparing with the other two logarithmic spiral failure surfaces as shown in Fig. 10a. Also from the figure, it seems to be that the modified Meyerhof's approach which considers the Rankine active stress zone above the pipeline is more consistent with the failure mechanism comparing with the traditional logarithmic spiral failure surface, after examining the glass window view of the pipe loading test by Audibert and Nyman[7], and thereby close to the measured results. It could confirm that the modified Meyerhof's approach is more agreeable to the behavior of oblique angle pipe in dense sand. The findings are compatible with the calculation for the passive earth pressure of retaining wall, in which the planar failure surface usually gives the higher values of passive earth pressure, whereas the logarithmic spiral surface seems to be more

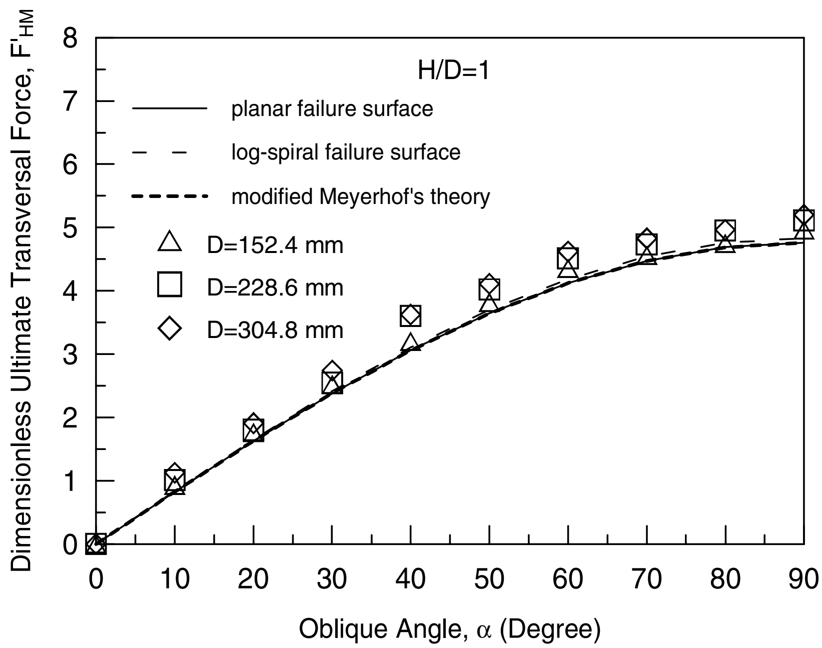

(a)

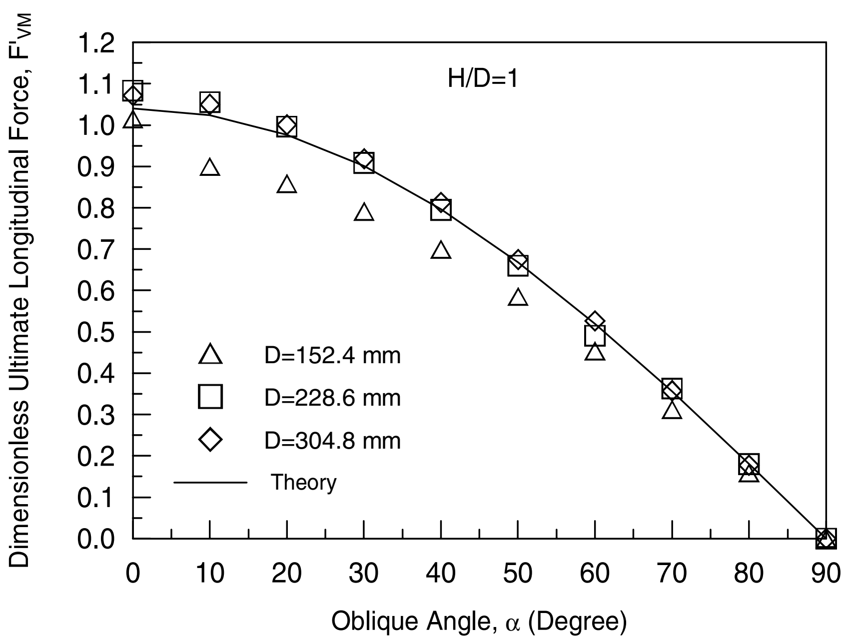

(b)

Fig. 8 Oblique Angle for Different Size Pipes with H/D = 1 versus: (a) Dimensionless Ultimate Transversal Force F'_{HM} and (b) Dimensionless Ultimate Longitudinal Force F'_{VM}

reasonable with the nature of the actual failure mechanism. Similarly, the longitudinal soil restraint could be computed through the force equilibrium with the multiplication of the corresponding cosine value of the oblique angle and the associated longitudinal soil restraint of the axial pipe (α = 0º). For comparison purposes, the longitudinal soil restraint of oblique pipe was converted into the dimensionless term of F'_{VM}. The theoretical predictions are in consistent agreement with the experiment results as shown in Figs. 8b, 9b, and 10b, respectively.

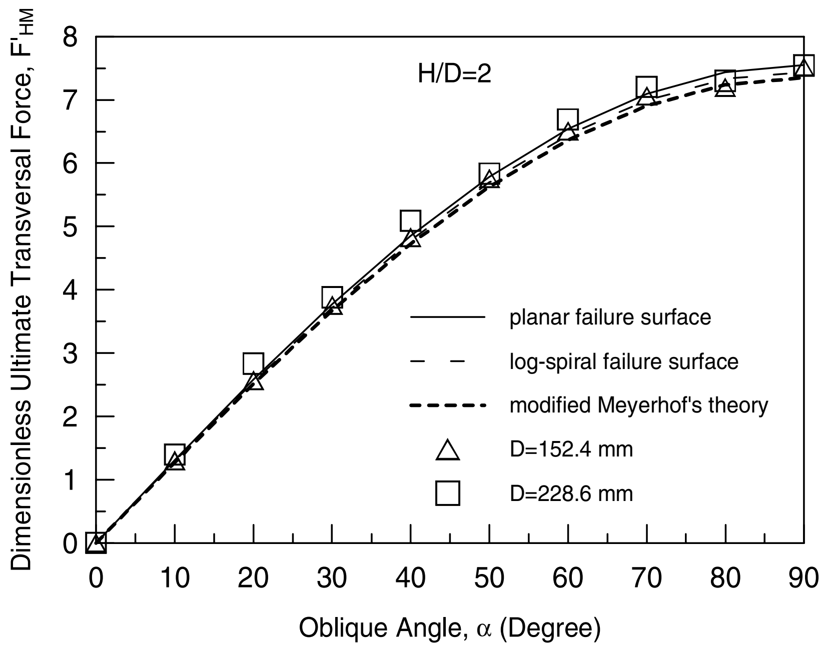

(a)

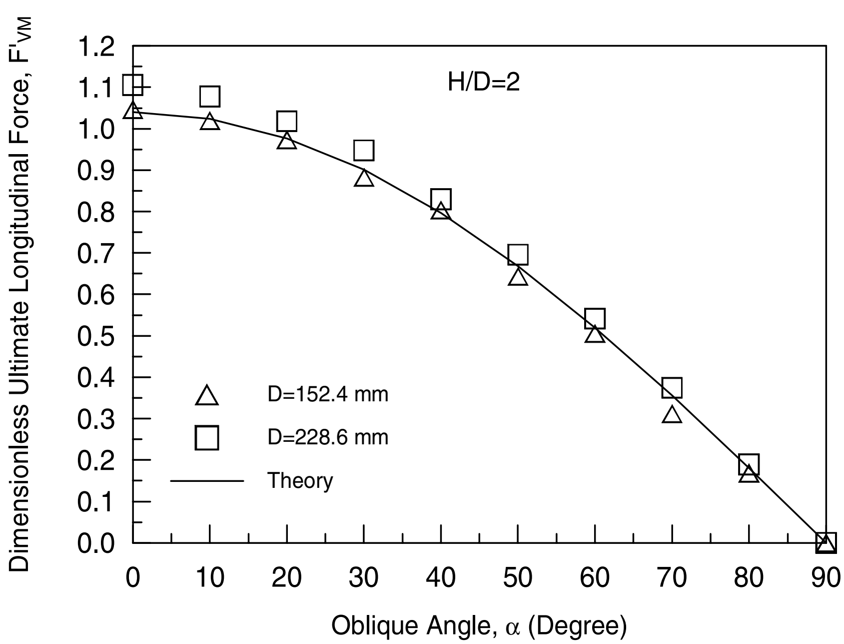

(b)

Fig. 9 Oblique Angle for Different Size Pipes with H/D = 2 versus: (a) Dimensionless Ultimate Transversal Force F'_{HM} and (b) Dimensionless Ultimate Longitudinal Force F'_{VM}

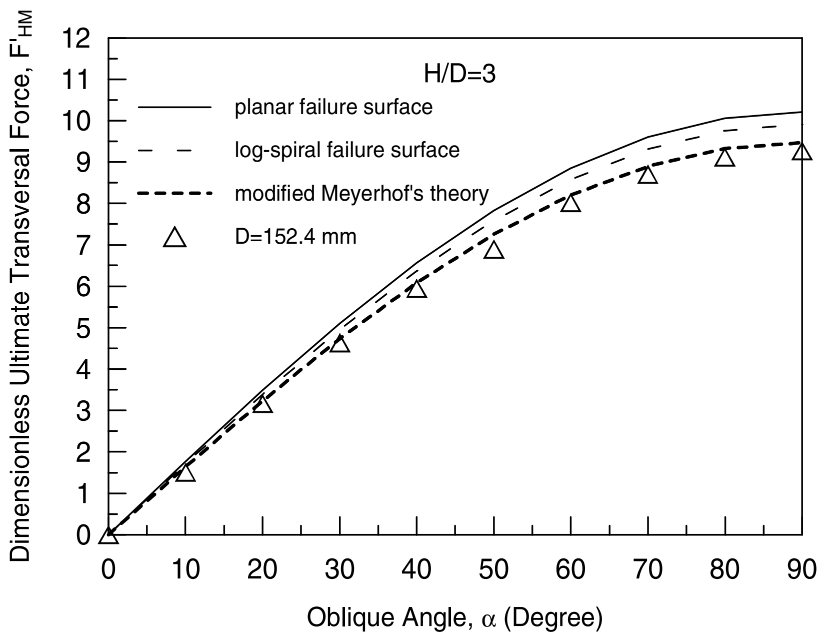

(a)

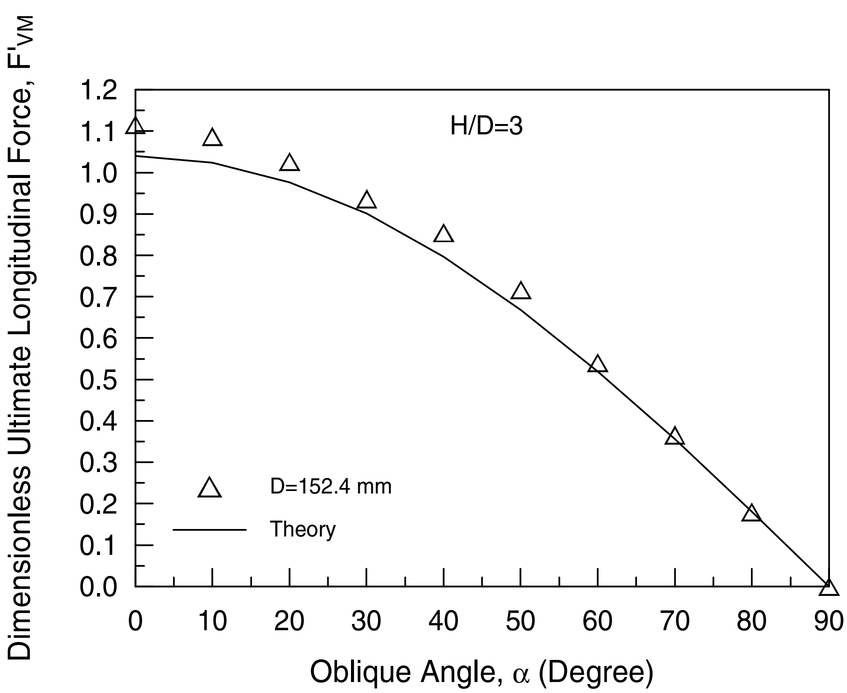

(b)

Fig. 10 Oblique Angle for Different Size Pipes with H/D = 3 versus: (a) Dimensionless Ultimate Transversal Force F'_{HM} and (b) Dimensionless Ultimate Longitudinal Force F'_{VM}

CONCLUSIONS

The results of an extensive series of experimental investigation on the soil friction restraint against the oblique motion of pipelines in dense sand are presented. Three different approaches to theoretically predict the associated transversal soil restraints of the oblique angle pipes are also proposed and compared with the experimental results. The following conclusions can be drawn. The longitudinal soil restraint of the axial pipe could be estimated as the product of the average of the vertical earth pressure and the horizontal earth pressure at rest at the pipe centerline and the tangent value of soil-pipe friction angle. For oblique angle pipes, the longitudinal soil restraint could be geometrically obtained by multiplying the corresponding cosine value of the oblique angle with the associated longitudinal soil restraint of the axial pipe. The transversal soil restraint of the oblique pipe could be obtained by multiplying the corresponding sine value of the oblique angle with the associated transversal soil restraint of the lateral pipe. For the lateral pipes, the modified Meyerhof's approach on the bearing capacity of foundation with assuming the logarithmic spiral failure surface was more close to the experimental results comparing with the planar sliding surface. The scale effects on the soil restraints were minor for the pipe diameter up to 304.8 mm.

ACKNOWLEDGMENT

This research was sponsored by the National Science Council of Taiwan under grant number NSC88-2611-E005-008. The writers are grateful for the financial support.

REFERENCES

1. Nyman KJ. “Soil response against oblique motion of pipes.” Journal of Transportation Engineering ASCE 1984; 110(2): 190-202.
2. O'Rourke MJ, Liu X, Flores-Berrones R. “Steel pipe wrinkling due to longitudinal permanent ground deformation.” Journal of Transportation Engineering ASCE 1995; 121(5): 443-451.
3. O'Rourke MJ, El Hmadi K. “Analysis of continuous buried pipelines for seismic wave effects.” Earthquake Engineering and Structural Dynamics 1988; 16(6): 917-929.
4. Brumund W, Leonards G. “Experimental study of static and dynamic friction between sand and typical construction materials.” Journal of Testing and Evaluation 1973; 1(2): 162-165.
5. Terzaghi K, Peck RK, Mesri G. “Soil mechanics in engineering practice.” 3rd edition, John Wiley and Sons, New York 1996: 417-445.
6. Hsu TW, Chen YJ, Wu, CY. “Soil friction restraint of oblique pipelines in loose sand.” Journal of Transportation Engineering ASCE 2001; 127(1): 82-87.
7. Audibert JME, Nyman KJ. “Soil restraint against horizontal motion of pipes.” Journal of the Geotechnical Engineering Division ASCE 1977; 103(GT10): 1119-1142.
8. Meyerhof GG. “Some recent research on the bearing capacity of foundations.” Canadian Geotechnical Journal 1963; 1(1): 16-26.
9. Meyerhof GG. “The bearing capacity of foundation under eccentric and inclined loads.” Proceedings of 3rd International Conference on Soil Mechanics and Foundation Engineering, Zurich, Swiss 1953; (1): 440-445.